HHS Public Access

Author manuscript

Dev Neurobiol. Author manuscript; available in PMC 2019 June 06.

Published in final edited form as:

Dev Neurobiol. 2018 November ; 78(11): 1064–1080. doi:10.1002/dneu.22629.

Caudal Transplantation of Ears Provides Insights into Inner Ear Afferent Pathfinding Properties

Clayton Gordy[1,2,3], **Hans Straka**[2], **Douglas W Houston**[1], **Bernd Fritzsch**[1], and **Karen L Elliott**[1]

[1]Department of Biology, University of Iowa, Iowa City, Iowa

[2]Department Biology II, Ludwig-Maximilians-University Munich, Planegg, Germany

[3]Graduate School of Systemic Neurosciences, Ludwig-Maximilians-University Munich, Planegg, Germany

Abstract

Numerous tissue transplantations have demonstrated that otocysts can develop into normal ears in any location in all vertebrates tested thus far, though the pattern of innervation of these transplanted ears has largely been understudied. Here, expanding on previous findings that transplanted ears demonstrate capability of local brainstem innervation and can also be innervated themselves by efferents, we show that inner ear afferents grow toward the spinal cord mostly along existing afferent and efferent fibers and preferentially enter the dorsal spinal cord. Once in the dorsal funiculus of the spinal cord, they can grow toward the hindbrain and can diverge into vestibular nuclei. Inner ear afferents can also project along lateral line afferents. Likewise, lateral line afferents can navigate along inner ear afferents to reach hair cells in the ear. In addition, transplanted ears near the heart show growth of inner ear afferents along epibranchial placode-derived vagus afferents. Our data indicate that inner ear afferents can navigate in foreign locations, likely devoid of any local ear-specific guidance cues, along existing nerves, possibly using the nerve-associated Schwann cells as substrate to grow along. However, within the spinal cord and hindbrain, inner ear afferents can navigate to vestibular targets, likely using gradients of diffusible factors that define the dorso-ventral axis to guide them. Finally, afferents of transplanted ears functionally connect to native hindbrain vestibular circuitry, indicated by eliciting a startle behavior response, and providing excitatory input to specific sets of extraocular motoneurons.

Keywords

Xenopus laevis; ear; transplantation; afferent innervation

INTRODUCTION

Afferents that develop from the inner ear establish precise connections between hair cells and central nuclei (Mao *et al.*, 2014; Fritzsch *et al.*, 2015; Goodrich, 2016). Within the central nervous system (CNS), these neurons terminate in anatomic and modality specific

Correspondence to: Karen L. Elliott (karen-elliott@uiowa.edu).

regions in the hindbrain: vestibular ganglion afferents reach vestibular nuclei and auditory afferents reach auditory nuclei (Maklad and Fritzsch, 2003; Fritzsch *et al.*, 2005a). To ensure the discrete processing of auditory and vestibular mechanical stimuli, growing afferents must correctly navigate within the CNS to reach selectively their target nuclei. The central navigational properties of developing inner ear afferents is incompletely understood (Maklad and Fritzsch, 2003), but can be partially derailed in mutants of certain transcription factors such as Neurod1 (Jahan *et al.*, 2010) and several others (Goodrich, 2016). In addition, afferent projections are established in a spatiotemporal progressing manner (Fritzsch *et al.*, 2005a; Zecca *et al.*, 2015) likely using Wnt gradients to navigate (Fritzsch and Elliott, 2017; Yang *et al.*, 2017) and can do so even if target nuclei are molecularly ablated (Elliott *et al.*, 2017).

In contrast to the ear, the molecular basis of the retinotopic projection of the eye is better understood in terms of Eph and ephrin gradients (Kullander and Klein, 2002; Liu *et al.*, 2016) to set up the chemoaffinity-mediated retinotopic map (Sperry, 1963). In addition, retinal afferents may be attracted to the midbrain as revealed by transplantation of a developing eye onto the spinal cord in *Xenopus laevis* embryos that showed fibers to reach the midbrain (Giorgi and Van der Loos, 1978). More recent work in transplanting an eye to the trunk demonstrated the ability of afferents to provide successful sensory input into the CNS, but did not reveal how afferent information reached the CNS (Blackiston *et al.*, 2017). Collectively, this suggests the possibility of long range cues acting in retinal ganglion cell afferent pathfinding. Additional work on olfactory transplantations suggest that olfactory afferents can navigate and interact with any nearby part of the brain, including the hindbrain but not the spinal cord (Stout and Graziadei, 1980; Klein and Graziadei, 1983; Magrassi and Graziadei, 1985).

As with eyes (Giorgi and Van der Loos, 1978; Blackiston *et al.*, 2017) and the olfactory system, transplantation of developing ears has long been used to demonstrate normal development in foreign positions (Yntema, 1955; Jacobson, 1963; Fritzsch *et al.*, 1998a; Swanson *et al.*, 1990). How ears compare to such transplantations with respect to homing to their targets has only been assessed for the hindbrain and midbrain: Transplantation of a third ear rostral to the native ear demonstrated afferent capability to enter the hindbrain and reach the vestibular nucleus (Elliott *et al.*, 2015a; Elliott *et al.*, 2015b) somewhat similar to retinal afferents ability to reach the midbrain in three eyed frogs (Constantine-Paton and Law, 1978) or eyes transplanted to the spinal cord (Giorgi and Van der Loos, 1978). In contrast, ear afferents reaching the midbrain could not navigate in any discernible patterns (Elliott *et al.*, 2013), suggesting that hindbrain navigation is guided by molecular cues that are not present in the midbrain, clearly distinct from retinal afferents coming from the spinal cord or the midbrain to extend under certain circumstances to the hindbrain (Manns and Fritzsch, 1991).

Previous work transplanting an ear caudally to the trunk has shown that inner ear afferents can enter the spinal cord (Elliott and Fritzsch, 2010); however, it remains unclear if ear transplantations near the spinal cord can successfully integrate sensory information as has been shown for eyes (Blackiston *et al.*, 2017). Given the above outlined ability of inner ear afferents to navigate to and within the hindbrain from altered entry positions, we investigate

here if inner ear afferents transplanted to the trunk can reach the vestibular nucleus in the hindbrain either through the spinal cord or through fasciculation along other peripheral nerves. We assess this capability through transplantation of ears at different developmental time points to various caudal locations on the animal, specifically both along the spinal cord or near the heart. Our data reveal that inner ear afferents can navigate either on their own or along peripheral nerves to reach the spinal cord and, if they grow along existing central fibers to the hindbrain, can reach vestibular nuclei once they reach the hindbrain. Physiological and behavioral data support that transplanted ear afferents establish meaningful connections with brainstem neurons to guide escape responses and provide excitatory input to specific sets of extraocular motoneurons.

MATERIAL AND METHODS

Animals

Xenopus laevis embryos of either sex were obtained through induced ovulation by injection of human chorionic gonadotropin, followed with fertilization by sperm suspension in 0.3X Marc's Modified Ringer's Solution (MMR, diluted from 10X stock; 1M NaCl, 18mM KCl, 20 mM $CaCl_2$, 10 mM $MgCl_2$, 150 mM HEPES, pH 7.6–7.8). The jelly coat was removed with 2% cysteine in 0.1X MMR. Embryos were incubated in 0.1X MMR until having reached the desired stage for manipulation (see below), and until desired stages for tracing, behavior, and physiological experiments (described below) as described by Nieuwkoop and Faber (1994).

Ear Transplantations

All surgical manipulations were performed in 1.0X MMR at room temperature. Animals were anesthetized with 0.02% Benzocaine (Crook and Whiteman, 2006) prior to and during all manipulations. Otic placodes and otic vesicles from donor embryos were removed and transplanted to recipient hosts at stage 25–27 and 28–36, respectively. Removed placodes or vesicles were grafted adjacent to the spinal cord in place of a removed somite on one side of the embryo. Additionally, otic vesicles from stage 32–36 donor embryos were transplanted to the ventral heart region, in the vicinity of the vagus nerve trajectory. Embryos were kept in 1.0X MMR after surgery for 15–30 min to allow healing. Animals were then transferred into 0.1X MMR. Animals to be used for behavioral and physiological assays were processed as below. Animals used only for immunohistochemistry and dye labeling were allowed to grow until stage 46, and subsequently anesthetized in 0.02% Benzocaine and fixed by immersion in either 4% paraformaldehyde (PFA), when used for immunohistochemistry or dextran tracing, or in 10% PFA when used for lipophilic dye tracing (see below). Successful development of the ear was confirmed at stage 46 based on the presence or absence of an ear in the region of transplantation and by the presence of otoconia. Ear development was further assessed using anti-Myo6 antibody to label hair cells and anti-tubulin antibody to label nerve fibers (see immunochemical analysis below). Only animals with fully formed transplanted ears, as indicated by otoconia in position above sensory epithelia, were used for further analysis.

C-start Startle Assay and Analysis

For startle response testing, donor ears were transplanted to the trunk at stage 25–27 as described above, but at a slightly more rostral position along the spinal cord. At stage 40–42, the native two ears were removed. For controls, both native ears were removed at stage 40 from animals that did not have an ear transplanted to the trunk. This time point of stage 40–42 was selected since nearly all Mauthner cells, the cells in the hindbrain that drive the c-start startle response from inner ear stimulation (Korn and Faber, 2005), survive with ear removal at stage 40 (Elliott *et al.*, 2015a). Animals were allowed to grow until stage 46. Tadpoles were placed individually in a 50 mm diameter Petri dish containing 0.1X MMR for the startle assay. Startle responses were elicited from dropping a 3.5 kg standardized object from a 12 cm height onto a sturdy lab bench, adjacent to the Petri dish containing the tadpole. Subsequent C-start startle response behavior was video recorded in slow-motion from a fixed distance directly above the Petri dish. Each of 13 control animals and 15 animals with transplanted ears were subjected to four trials and the presence or absence of a response, as well as the initial direction of the response, if present, was documented. Significance of direction of turn (Zarei *et al.*, 2017) was calculated using a Chi-Square analysis with Microsoft Excel. Following behavioral analysis, animals were anesthetized in 0.02% Benzocaine and fixed by immersion 10% PFA as described above and were then processed for lipophilic dye labeling.

Electrophysiology

Following ear transplantations at stage 28–29 (see above), *Xenopus laevis* tadpoles of either sex were obtained from the in-house animal breeding facility at the Biocenter-Martinsried at the Biomedical Center of the Ludwig-Maximilians-University Munich. Tadpoles were kept in tanks filled with 17–18°C non-chlorinated water at a 12/12 light/dark cycle. A total of 5 animals at developmental stages 54–57 were used for recordings of neuronal activity. Experiments were performed *in vitro* on isolated, semi-intact preparations and comply with the National Institute of Health publication entitled “Principles of animal care,” No. 86–23, revised 1985. Permission for these experiments was granted by the governmental institution at the Regierung von Oberbayern/Government of Upper Bavaria (55.2–1–54–2532–14–2016; 55.2–1–54–2532.0–24–2017).

For all experiments, tadpoles were anesthetized in 0.05% 3-aminobenzoic acid ethyl ester (MS-222; Pharmaq Ltd., United Kingdom) in frog Ringer (75 mM NaCl, 25 mM NaHCO3, 2 mM CaCl2, 2 mM KCl, 0.5 mM MgCl2, and 11 mM glucose, pH 7.4) and decapitated ~10 segments below the transplanted ear. The skin above the head was removed, the skull and rostral vertebrae opened, and the forebrain disconnected. This surgical procedure preserved all inner ear organs, the CNS and the extraocular motor innervation and allowed natural and galvanic stimulation of vestibular endorgans and recording of extraocular motor responses (Gensberger *et al.*, 2016).

Extracellular multi-unit spike discharge from severed extraocular motor nerves was recorded with glass suction electrodes from the cut end of the extraocular motor nerves as described earlier (Lambert *et al.*, 2008). Glass microelectrodes were made with a horizontal puller (P-87, Sutter Instruments Co., USA) and were individually adjusted at the tip to fit the

diameter of the respective target nerves. Extraocular motor nerve activity was recorded (EXT 10–2F; npi electronic GmbH, Germany), digitized at 10–20 kHz (CED 1401, Cambridge Electronic Design Ltd., United Kingdom), and stored on a computer for offline analysis. For the analysis, responses obtained during 20–120 repetitions of sinusoidal turntable oscillations or sinusoidally modulated current stimuli (see below) were averaged to obtain the mean response ± standard error of the mean (SEM) over a single cycle.

Motion and Galvanic Vestibular Stimulation

The recording chamber with the semi-intact *Xenopus* preparations was mounted on a computer-controlled, motorized two-axis turntable (ACT-1002, Acutronic USA Inc., Switzerland) with the preparation centered in the horizontal and vertical rotation axes to provide optimal activation of semicircular canal organs (Gensberger *et al.*, 2016; Lambert *et al.*, 2008). Motion stimuli consisted of sinusoidal rotations across frequencies that ranged from 0.2 to 1 Hz (peak velocities: ±12–60°/s). Sinusoidally modulated galvanic currents were applied by stimulus electrodes that consisted of two Teflon-coated silver wires (diameter: 0.76 mm; AG 25-T, Science Products GmbH, Germany), placed on the outer surface of the native otic capsules or the transplanted third ear. The two stimulus electrodes were cut at the tip, chlorinated to minimize polarization, and separately attached to a micromanipulator, to enable precise positioning under visual guidance. For most experiments, electrodes were placed bilaterally in close proximity of the visible cupulae of a specific bilateral coplanar semicircular canal pair (e.g., left posterior and right anterior semicircular canal). To stimulate the third ear, one electrode was placed on the outer surface of the visible otic capsule and the second electrode at a distance of ~10 mm from the first in the Ringer solution of the recording chamber. Sine waves for the galvanic vestibular stimulation (GVS) were produced with a linear stimulus isolator (WPI A395, World Precision Instruments Inc., USA), triggered by the analog output from an analog/digital converter (CED 1401). The galvanic currents were applied to the two electrodes in phase-opposition (Gensberger *et al.*, 2016) and consisted of sinusoidally modulated currents at frequencies of 0.2–1 Hz and magnitudes of ±50–200 μA for GVS of the native semicircular canals and of ±200–500 μA for GVS of the third ear.

Lipophilic Dye Labeling

Axonal projections from transplanted ears were labeled using NeuroVue lipophilic dyes (Fritzsch *et al.*, 2016a). NeuroVue™ Maroon, NeuroVue™ Red, and NeuroVue™ Jade (Polysciences, Inc.) dye-soaked filter paper pieces were cut to fit and were placed inside transplanted ears. Care was taken to place the dye on regions of sensory epithelia as determined by location of otoconia. Dye placed in transplanted ears labels inner ear afferent axons through backfilling of dendritic processes, terminating on hair cells, into ganglion cell bodies. Dye was also placed into the spinal cord following transection, either rostral or caudal, to the adjacently transplanted ear to fill inner ear afferent axonal processes within the spinal cord as they project within it and into the hindbrain. To determine lateral line innervation of an ear transplanted adjacent to the spinal cord, dye was placed into the posterior lateral line ganglia caudal and adjacent to the native ear, filling lateral line afferents to neuromast (lateral line) organs along the trunk of the animal. In the same animals, dye was placed into the spinal cord to label afferents entering the CNS. Native ear afferent

projections into the hindbrain were labeled with dye inserted into each native ear. Following dye insertions, animals were kept in 0.4% PFA and incubated at 60°C or 36°C to permit diffusion. Dye placed in the spinal cord or posterior lateral line ganglia were incubated at 60°C for 60 hr. Dye placed into transplanted ears near the spinal cord were incubated for 18 hr at 36° to determine the spinal cord entry point or for 60 hr at 60° to assess hindbrain innervation. Ears transplanted to the heart region were labeled with dye insertions either into the transplanted ear or into the vagus nerve directly and were incubated for 3 days at 60°. Native ear dye placements were incubated for 18 hr at 36°. Following diffusion, the brain and spinal cord was dissected out and the specimens were mounted in glycerol for imaging on a TCS SP5 Multi-photon confocal microscope using excitation emission settings specific for the different lipophilic dyes used (Tonniges *et al.*, 2010).

Dextran amine Labeling

Dextran amine dye injections into ears transplanted adjacent to the spinal cord were used to evaluate inner ear afferent projection in the CNS. Entry points of inner ear afferents into the spinal cord as well as their projections into the hindbrain were evaluated using Texas red, tetramethylrhodamine, Alexa Fluor 647, and Alexa Fluor 488 dye (Molecular Probes). A small incision was made into the transplanted ear of anesthetized animals (0.02% Benzocaine) and a recrystallized drop of the labeling dye on a tungsten needle was inserted (Fritzsch, 1993). Care was taken to fill the ear entirely with the dye. Animals were washed in 0.1X MMR three times in succession and kept in a dish containing 0.1X MMR for 2–3 hr. Afterwards, the embryos were reanesthetized in 0.02% Benzocaine and fixed in 4.0% PFA. After fixation, the brain and spinal cord was dissected out and the specimens were mounted in glycerol for imaging on a TCS SP5 Multiphoton confocal microscope using appropriate excitation/emission filter settings. Dextran amine tracing served to verify lipophilic dye tracing as it is not known to diffuse transcellularly.

Immunohistochemistry

To determine presence of sensory epithelia in transplanted ears, as well as local innervation of the ear and its surroundings, PFA fixed stage 46 animals were dissected to remove the lower jaw and skin and were dehydrated in 70% ethanol overnight. Animals were washed in 1X PBS three times for 10 min each before being blocked in 5.0% normal goat serum (NGS) with 0.1% Triton-X 100 for 1 hr. Following a brief wash in 1X PBS, primary antibodies against neuronal marker acetylated tubulin (1:800, Cell Signaling Technology) and against hair cell marker Myosin VI (1:400, Proteus Biosciences) were incubated with the embryos overnight at 36°C. Animals were washed thrice for 10 min and blocked in 5.0% NGS + 0.1% Triton X 100 for 1 hr prior to incubation with speciesspecific secondary antibodies (1:500, Alexa) along with nuclei marker Hoechst 33342 (Invitrogen) overnight. Animals were washed in 1X PBS six times for 15 min each and mounted in glycerol for imaging on a TCS SP5 Multi-photon confocal microscope. In animals where neuromast organs and lateral line afferents were of interest, the skin was kept on during the procedures listed above.

Three-Dimensional Reconstructions

Three-dimensional reconstructions were made from confocal images as previously described (Kopecky *et al.*, 2012). Briefly, ears transplanted to the trunk that were immunostained for

tubulin and MyoVI as described above were mounted with the trunk lateral side up on a microscope slide in glycerol. In addition, brains from animals in which the transplanted and native ears or the spinal cord and native ears were labeled with lipophilic dye as described above were removed, hemisected along the midline and mounted lateral side up on a slide in glycerol. Confocal z-series images were taken using a Leica TCS SP5 confocal microscope. Z-series stacks were loaded into Amira software (Version 5.4) for manual segmentation, as previously described (Kopecky *et al.*, 2012). Fibers were individually traced and reconstructed as previously described for dendrites (Elliott *et al.*, 2015a)

RESULTS

Success and Development of Transplantations

Success of transplantations was assessed based on the presence and degree of development of an ear with otoconia at the place of transplantation (Table 1, Fig. 1A–C). While most transplants were successful in that they developed ears with otoconia, in some instances ears developed without otoconia or formed otoconiafree vesicles (Table 1), consistent with data from similar placements adjacent to the spinal cord to assess the ability of spinal motor neurons to become efferents to inner ear hair cells (Elliott and Fritzsch, 2010). Similar rates of success were found for ears transplanted adjacent to the spinal cord and ventrally near the heart; 83 and 84 percent of animals had transplanted ears with otoconia, respectively (Table 1, Fig. 1). Only ears that contained otoconia were used for further analysis as presence of otoconia always coincides with hair cell formation (Elliott and Fritzsch, 2010). Transplanted ears containing otoconia were examined for degree of development by immunostaining with antibodies against MyoVI and acetylated tubulin, markers for hair cells and neurons, respectively. Positive MyoVI staining revealed the presence of hair cells in transplanted ears (Fig. 1F). Hair cells were found to be in discrete clusters within the ear, indicating distinct vestibular end-organ sensory epithelia formation consistent with near normal ear development. Additionally, tubulin identified neurons and their processes associating with sensory epithelia in the transplanted ears (Fig. 1F). These results indicate that ears transplanted in this study are capable of developing hair cells and neurons, similar to those present in native ears and consistent with past work (Harrison, 1935; Yntema, 1955; Fritzsch *et al.*, 1998a).

Entry and Projection of Afferents in Ears Transplanted to the Spinal Cord

Since ear afferent connections with the spinal cord in identical transplants have been observed previously by retrograde labeling of ganglion cells from dye injection into the spinal cord (Elliott and Fritzsch, 2010), as well as in this study (Fig. 2A,E–F), afferent axon projections into the spinal cord were traced from the ear using lipophilic or dextran amine dyes (Fritzsch, 1993; Fritzsch *et al.*, 2005b). We aimed to determine if inner ear afferents from an ear transplanted adjacent to the spinal cord enter and project dorsally in the spinal cord as native afferent fibers do in the hindbrain.

Following labeling of afferent projections from the ear, the brain and spinal cord were dissected from the embryo and the entry point along the dorsal-ventral (D-V) axis of the spinal cord was determined (Fig. 2B–D). In assigning the D-V plane of entry, confocal

scanning of the spinal cord along the entire D-V plane was used to define a midline position, where the middle of the z-series stack was considered neither dorsal nor ventral, while labeled afferents observed above or below this midline were considered to be dorsal and ventral entering, respectively (Fig. 2D). The majority of cases (14/20; 70%) had projections with a dorsal entry point, whereas five animals showed a ventral entry point and one animal had afferents enter at the midline (Fig. 2D′).

Plane of fiber projection within the spinal cord was assessed in a similar manner and was defined by the D-V plane where fibers were observed to project once inside the spinal cord. Regardless of entry point, all 20 animals examined had afferents projecting dorsally within the spinal cord (Fig. 2D′). Additionally, these projections extended both rostral and caudal from the entry site. These results suggest that similar cues guide inner ear afferents in the hindbrain and spinal cord, consistent with known molecular conservation of dorso-ventral patterning in these areas of the CNS (Fritzsch *et al.*, 2006; Fritzsch and Elliott, 2017).

Ears Transplanted Adjacent to the Spinal Cord Project to the Hindbrain

Since ear afferent projections into the spinal cord appear to project dorsally regardless of entry point (Fig. 2), we next sought to identify if the afferent fibers projected into the hindbrain, and once within, if connections are established with the dorsally located vestibular nucleus, extending beyond past research showing such projections after ear transplantations adjacent to the hindbrain itself or adjacent to cranial nerves projecting to the hindbrain (Elliott *et al.*, 2013; Elliott *et al.*, 2015b). In control animals, dye injection into the spinal cord (Fig. 3A) labels all ascending spinal tracts as well as trigeminal (V) nucleus afferents in the hindbrain (Fig. 3A′–B, green), as there exists a continuity between the hindbrain located descending tracts of V and ascending spinals (Maklad and Fritzsch, 2003). In animals with an ear transplanted next to the spinal cord, dye injection into the transplanted ear (Fig. 3C) also label dorsal ascending spinal tracts, as well as trigeminal tracts in the hindbrain (Fig. 3C′–D), suggesting that afferents from the transplanted ear fasciculate with ascending spinal tracts to enter the hindbrain and further continue along centrally located trigeminal tracts (Fig. 3C′–D).

To determine whether these afferents from transplanted ears terminated in the dorsally located vestibular nucleus, dye was implanted into the native ears to label the vestibular nucleus (Fig. 3, red), providing a reference point with which to assess if transplanted inner ear afferents reroute from the more ventrally located trigeminal tracts they project with upon entering the hindbrain. In these transplanted ear animals, fibers apparently rerouted from the trigeminal tracts and into the vestibular nucleus upon reaching the hindbrain (Fig. 3C′–D″). Given the well-defined positions of sensory tracts and nuclei along the alar plate (Fritzsch *et al.*, 2005a), closer examination showed that all 8 animals had fibers approaching and/or projecting directly into the vestibular nucleus. In contrast, in 8 control animals, no fibers from the spinal labeled tracts and hindbrain trigeminal tracts display any rerouting into the vestibular nucleus (Fig. 3A′–B″). Collectively these data show that inner ear afferents that enter the hindbrain from the spinal cord are capable of projecting to the vestibular nucleus, suggesting vestibular afferents are being navigationally instructed through yet unknown molecular cues once entering the hindbrain.

Transplanted Ears Make Functional Connections With The Hindbrain

To determine whether the inner ear afferents that reach the vestibular nucleus are making functional connections, behavioral and functional assays were conducted. To test for functional connections between the inner ear afferents of the transplanted ear and a second-order neuron in the vestibular nucleus of the hindbrain, the Mauthner cell (Korn and Faber, 2005), we utilized a C-start startle assay (Zarei *et al.*, 2017). We tested 13 control animals in which both native ears were removed, thus lacking any inner ear input, and 15 animals in which both native ears were removed but had an ear transplanted adjacent to the spinal cord. Native ear removals were performed between stages 40–42 to ensure survivability of the Mauthner cells (Elliott *et al.*, 2015a). Attempts to elicit a C-start startle response in the thirteen control animals lacking all ears were unsuccessful (Fig. 4A). In contrast, in animals with an ear transplanted to the spinal cord and the native ears removed, eliciting a C-start startle response was successful in five of fifteen animals (Fig. 4A). Of these five animals, one animal responded in all four trials, one responded in two of four trials, and three animals responded in one of four trials. Of these nine trials that had responses, eight resulted in turns away from the transplanted ear and only one toward (Fig. 4A′). This was significantly different from an expected absence of directional bias ($P < 0.05$). Given that wild type animals with both native ears turn in either direction with equal probability and those with one ear removed turn away from the remaining ear nearly every time (Zarei *et al.*, 2017), our data suggest that the ears transplanted adjacent to the spinal cord can develop functional connections within the vestibular nucleus that direct the movement of the tadpole away from the incoming stimulus from that ear. Furthermore, lipophilic dye tracing (Fig. 4B) of transplanted ears in these animals revealed inner ear afferents navigating to the vestibular nucleus in those animals that responded. In fact, the animal that responded in all four trials was the only one that had robust innervation of the ipsilateral vestibular nucleus and to a lesser degree, the contralateral vestibular nucleus (Fig. 4C–4E). This may explain why this animal had three turns away from the transplanted ear and one turn toward the transplanted ear. In addition, the Mauthner cell could be transcellularly labeled through the transplanted ear afferents (Fig. 4C), further supporting physical and functional contacts of these afferents with second-order neurons in the vestibular nucleus.

Further validation of functionally adequate synaptic wiring was examined by testing the connectivity of the transplanted ear with the vestibulo-ocular reflex (VOR) circuitry. Semi-intact *in vitro* preparations (Straka and Simmers, 2012) of animals at stage 53–57 ($n = 5$) with a transplanted third ear were employed to test the performance of the VOR during natural motion (Lambert *et al.*, 2008) and GVS of native and ectopic inner ears (Gensberger *et al.*, 2016). After disconnection from the target eye muscle, multi-unit spike discharge of various extraocular motor nerves ($n = 15$), such as the inferior rectus (IR) nerve were recorded (Fig. 5A,B). The multi-unit discharge of all recorded extraocular motor nerves (mean resting rate ± SE: 28.7 ± 3.8 spikes/s; $n = 15$) was cyclically modulated during spatially specific sinusoidal rotation (1 Hz and ± 2° position oscillation; Fig. 5A). The multiunit firing rate of the IR nerve for example (Fig. 5C) oscillated during sinusoidal turntable motion along a plane formed by the ipsilateral anterior (iAC) and contralateral posterior semicircular canal (cPC). In this case, the discharge modulation was due to a robust excitatory component from the cPC (peak discharge: 60–90 spikes/s; Fig. 5D). A

comparable discharge modulation was obtained by sinusoidal GVS (1 Hz and ± 200 μA) of the same native bilateral semicircular canal pair, i.e., the iAC and cPC (Fig. 5E,F). The peak discharge occurred during galvanic depolarization of the cPC (Fig. 5F), complied with the prediction from the phase relationship of the spike firing during motion stimulation (Fig. 5D), and outlined the connectivity of the underlying VOR circuitry between the bilateral inner ear and the IR eye muscle (Straka *et al.*, 2014).

Given that motion stimulation activates vestibular endorgans in native ears as well as the ectopic ear, we applied sinusoidal GVS exclusively to the transplanted ear (Fig. 5A) to evaluate if the transplanted ear is functionally connected to the native VOR circuitry. In 10 out of 15 extraocular motor nerves recorded in 5 animals, sinusoidal GVS of the transplanted ear provoked a modulation of the spontaneous multi-unit discharge as exemplified for the contralateral IR nerve (Fig. 5G,H). The discharge modulation was robust across most trials (Fig. 5G) with a mean peak discharge (± SE) of 23.3 ± 4.2 spikes/s (n = 10). At variance with sinusoidal GVS of the native inner ears, the modulation consisted exclusively of an excitatory component as indicated by the lack of a firing rate disfacilitation (blue line in Fig. 5H). Also, the current intensity necessary to evoke a modulated discharge was higher for the transplanted ear (± 300 μA) compared to the native ears (± 100 μA). Most importantly, however, the peak discharge coincided with the depolarization of the cPC epithelium (green dotted line in Fig. 5H), confirmed by trials with inversed current polarities. This clearly indicates that the transplanted ear functionally links with excitatory vestibulo-ocular projection neurons known to form connections with contralateral extraocular motoneurons as the major driving force for the semicircular canal-dependent VOR. The failure to induce a discharge modulation of ipsilateral extraocular motoneurons by galvanic stimulation of the ectopic inner ear (5 out of 15 extraocular motor nerves) clearly indicates that the transplanted ear is exclusively connected to excitatory VOR pathways.

Collectively, the results obtained from testing the connectivity that arises from the transplanted ear suggests that afferent projections to hindbrain neuronal targets are indeed functionally meaningful. Additional work will define rules and constraints for integrating spinal cord-derived vestibular inputs into synaptic computations performed in native neural networks.

Fasciculation with Peripheral Nerves

Following a placodal origin in close proximity to native ears, pLL primordia migrate caudally toward the trunk and are found along the dorsal fin at stage 40 (Nieuwkoop and Faber, 1994). Given the caudal placement of the transplanted ear adjacent to the spinal cord, we next sought to identify if there would be an interaction with neurosensory components of the posterior lateral line (pLL) system. Specifically, are inner ear afferents able to navigate along the lateral line nerve and could lateral line afferents innervate the transplanted ear (Fritzsch *et al.*, 1998b)? Dye was placed into the pLL ganglia itself and into the pLL nerve caudal to the transplanted ear (Fig. 6A).

Afferents of the pLL were observed to innervate the skin above the transplanted ear as well as continue a caudal trajectory past the ear along the dorsal fin (Fig. 6B), unlike in native

ears where the skin above the ear is devoid of lateral line (Elliott and Fritzsch, 2010). Furthermore, pLL afferents were found to innervate the transplanted ear (Fig. 6B, arrowheads), as no inner ear ganglia were detected with the lipophilic dye from this injection. Placement of dye caudal to the transplanted ear, in the pathway of a more caudal segment of the pLL nerve, labeled inner ear ganglion cells (Fig. 6C), suggesting fasciculation between inner ear and pLL afferents. Furthermore, this caudal injection revealed innervation of the transplanted ear (Fig. 6C, arrowheads), most likely by inner ear afferents given the labeling of ganglia, though additional contribution of lateral line afferents to the innervation cannot be ruled out. Injection of dye directly into the spinal cord (Fig. 6A) labeled many more afferents and associated ganglia (Fig. 6D) than was labeled with a caudal application to the pLL nerve (Fig. 6C), though some afferents were labeled with both spinal cord and caudal lateral line dye applications (Fig. 6E). These data suggest that afferents of the inner ear are capable of projecting with peripheral nerves but do so as undirected growth along existing peripheral nerves.

To further test the possibility of fasciculation with any peripheral nerve bundles, we transplanted the ear ventrally into the region of the developing heart (Figs. 1C–D, 7B–C). Dye injections into the transplanted ear (Fig. 7A) identified afferents of the inner ear projecting with the vagus nerve (Fig. 7B). Furthermore, placement of dye into the vagus nerve (Fig. 7A) labeled ganglion cells of the transplanted ear, as well as their associated peripheral processes into the ear (Fig. 7C). These results further suggest that afferents of the inner ear are capable of fasciculation with any nearby peripheral nerve and that this potentially may be occurring without instructive signaling from nearby CNS sources.

DISCUSSION

Past research has demonstrated that various cranial sensory organs can be transplanted and develop normally even if not associated with their specific area of the brain (Yntema, 1955; Jacobson, 1963; Swanson *et al.*, 1990). Evidence indicates that several of these transplanted sensory organs can establish contact with the brain. Importantly, transplanted eyes and ears can project and interact with native projections to form columns of fibers suggestive of a compromise between molecular cues and activity (Constantine-Paton and Law, 1978; Elliott *et al.*, 2015b). Furthermore, retinal afferents may home to the midbrain from the spinal cord (Giorgi and Van der Loos, 1978) or may bring their information through unclear routes to the CNS (Blackiston *et al.*, 2017). The olfactory system seems to show no homing to a specific part of the brain but rather interacts with whatever brain area they reach (Stout and Graziadei, 1980; Morrison and Graziadei, 1983; Magrassi and Graziadei, 1985) possibly using the molecular guidance cues inherent to different olfactory receptors (Mombaerts *et al.*, 1996).

Transplanted ears have thus far only been analyzed regarding their homing behavior within the CNS if transplanted near the hindbrain or the midbrain. In the hindbrain, inner ear afferents navigate to reach the vestibular nuclei no matter their entry point and interact with native afferents (Elliott *et al.*, 2015b). In contrast, inner ear afferents project in a highly variable pattern into the midbrain, implying little to no guidance cues in this foreign territory (Elliott *et al.*, 2013). Our data provide clear evidence that the spinal cord allows inner ear

afferents to navigate to a dorsal position comparable to the hindbrain (Figs. 2 and 3), strikingly unlike the midbrain. This distinction may be owing to a stronger effect of dorso-ventral patterning molecular cues in the hindbrain and spinal cord, including Shh, Wnt, and BMPs, whereas the midbrain may require additional signals from the isthmus that alter navigation (Fritzsch *et al.*, 2006; Hernandez-Miranda *et al.*, 2016; Lai *et al.*, 2016; Fritzsch and Elliott, 2017; Glover *et al.*, 2018). While inner ear afferents entering the spinal cord project along the dorsal funiculus both in caudal and rostral directions, afferents that reach the hindbrain can form collaterals that reach the vestibular nuclei, overlapping with native projections, much like inner ear afferents reaching the hindbrain when transplanted adjacent to the native ear (Elliott *et al.*, 2015b). This suggests that molecular cues in the hindbrain, possibly associated with the Wnt signaling pathway that drives dorsally directed cochlear collaterals (Yang *et al.*, 2017), drive inner ear afferent collaterals to expand outside the trigeminal afferent fascicles to reach the vestibular nuclei. This ability to navigate in an as of yet incompletely understood molecular gradient seems also to allow inner ear afferents to navigate dorsally in the spinal cord, even if they entered ventrally. Our data thus suggest that a shared molecular patterning system guides inner ear afferents in the hindbrain and spinal cord and that this system is absent in the midbrain, explaining the random afferent trajectories in the latter (Elliott *et al.*, 2013) and the targeted projections in the former [Fig. 3 and (Elliott *et al.*, 2015b)]. There is no strong evidence that these molecular cues act over long distances to attract spinal cord entering afferent fibers as suggested for transplanted eyes (Giorgi and Van der Loos, 1978). Rather, it appears that fasciculation along existing dorsal root fibers, equally sorted by possibly the same gradient (Lai *et al.*, 2016), may by chance guide some afferents within the reach of local cues in the hindbrain that can diverge them to reach vestibular nuclei.

Inner ear afferents either directly labeled through dye injection into the ear (Figs. 2 and 3) or filled from the spinal cord (Fig. 2) show mostly a directed growth toward the spinal cord. This could simply be so because other earlier routes taken by various fibers have been eliminated between our transplantation time and observation time. Whether this apparent targeted growth of inner ear afferents to the spinal cord is due to neurotropic attractive interactions (fibers are specifically attracted to the spinal cord or more generally to the CNS) or due to neurotrophic interactions (early fibers that reached areas without proper support were eliminated) requires additional work on various early stages after transplantation. However, our data suggest that inner ear afferents prefer to fasciculate with existing nerves (Fig. 3). This observation is particularly obvious in the case of the lateral line nerve fibers, where such afferents can innervate the transplanted ear (Fig. 6) presumably by being supported through hair cell released neurotrophins such as BDNF that appear to be common to all hair cells (Fritzsch *et al.*, 2016b; Hallböök *et al.*, 2006). Likewise, inner ear afferents that navigate along lateral line afferents to reach neuromasts could be supported by BDNF released from neuromast hair cells. For the lateral line/inner ear afferent interactions there is random, non-directed growth along each other which appears to be not corrected for. This follows from data suggesting that neurotrophic support via common molecules released from inner ear/lateral line hair cells rescues the random growth of inner ear afferents toward the tail-ward neuromasts (Fig. 6). Obviously, these inner ear afferents have no chance of ever reaching the hindbrain These data are consistent with previous preliminary reports on

afferent growth to the spinal cord (Elliott and Fritzsch, 2010) or along lateral line nerves (Fritzsch *et al.*, 1998b; Fritzsch, 1999).

Epibranchial placode-derived neurons are unique in that they not only express the neurotrophin receptor TrkB but also express BDNF (Fritzsch *et al.*, 1997; Patel *et al.*, 2010). Inner ear afferents growing along the epibranchial placode-derived vagus afferents should thus fasciculate with that nerve. Our data of ear transplantation near the heart show that inner ear afferents fasciculate along the vagus nerve without any apparent deviation, indicating that neurotrophic survival support combined with fasciculation along Schwann cells suffices for an apparently directed growth of inner ear afferents along the vagus nerve toward the brain.

As a result of the observed capability to reroute into the vestibular nuclei, afferents from the spinal cord transplanted ear make functional connections with vestibular brainstem circuitry (see Fig. 5G,H). The modulated discharge of the majority of extraocular motor nerves during GVS clearly indicates that afferents from the transplanted ear form non-selective, ubiquitous excitatory connections with second-order vestibular neurons. However, the supplemental ocular motor activation trough central vestibular neurons is obviously restricted to excitatory VOR neurons, since a discharge modulation is only observed in extraocular motoneurons that are located contralateral to the transplanted ear. This connectivity pattern complies with the crossed excitatory circuit component of the native VOR that forms the dominant part of the classical push-pull organization (Straka *et al.*, 2014). This interpretation also corroborates the responses of tadpoles subjected to the startle assay that revealed a biased turn away from the ear, indicating that stimulation of the transplanted ear facilitates an excitation of the Mauthner cell (Fig. 4).

The ubiquitous excitation of hindbrain vestibular neurons including the Mauthner cell is not too surprising but appears to challenge the functionality of the connections. While a general activation of central vestibular neurons by afferents from the transplanted ear might be detrimental for the spatial specificity of the VOR, it is more likely not, given the presence of concurrent powerful afferent inputs from the native ears. In fact, a comparable situation has been described in adult ranid frogs after a partial loss of the VIIIth nerve (Goto *et al.*, 2001; Rohregger and Dieringer, 2003). Part of the post-lesional vestibular reorganization included an expansion of excitatory connections from the remaining intact afferent fibers onto functionally “incorrect” central vestibular neurons that have lost their peripheral inputs. The formation of such inappropriate connections that ensure the survival of the deafferented neurons was compensated by remaining adequate connections that guaranteed the maintenance of spatially appropriate reflexes. Thus, together, our results indicate that the hindbrain exhibits a remarkable plasticity in response to integrating rerouted novel vestibular inputs from the spinal cord. Nonetheless, further work is required to identify proper conditions that increase the efficacy of innervation from ectopic ear placements and the connectivity with functionally appropriate circuit components (Blackiston *et al.*, 2017). Our data imply that vestibular (and possibly auditory) connections can be made from transplanted ears to guide respective modality-specific behaviors.

Acknowledgements

This material is based upon work supported by the NASA Iowa Space Grant Consortium under Grant No. NNX10AK63H. KE is supported by an NIH R03 (DC015333). The authors acknowledge financial support by the Collaborative Research Center (CRC 870) and the Research Training Group (RTG 2175) of the German Science Foundation. The use of the Leica TCS SP5 multi-photon confocal microscope was made possible by a grant from the Roy. J. Carver Charitable Trust. The authors wish to thank K. Gensberger for technical help with initial electrophysiology experiments. We also thank the Office of the Vice President for Research (OVPR) of the University of Iowa for support. The authors have no conflicts of interest to declare.

Contract grant sponsor: NIH R03; contract grant number: DC015333.

Contract grant sponsor: NASA Iowa Space Grant Consortium; contract grant number: NNX10AK63H.

Contract grant sponsor: German Science Foundation; contract grant number: CRC 870, RTG 2175.

REFERENCES

Blackiston DJ, Vien K and Levin M (2017) Serotonergic stimulation induces nerve growth and promotes visual learning via posterior eye grafts in a vertebrate model of induced sensory plasticity. NPJ Regenerative Medicine, 2, 8. [PubMed: 29302344]

Constantine-Paton M and Law MI (1978) Eye-specific termination bands in tecta of three-eyed frogs. Science, 202(4368), 639–641. [PubMed: 309179]

Crook AC and Whiteman HH (2006) An evaluation of MS-222 and benzocaine as anesthetics for metamorphic and paedomorphic tiger salamanders (Ambystoma tigrinum nebulosum) The American Midland Naturalist, 155, 417–421.

Elliott KL and Fritzsch B (2010) Transplantation of Xenopus laevis ears reveals the ability to form afferent and efferent connections with the spinal cord. The International Journal of Developmental Biology, 54(10), 1443–1451. [PubMed: 21302254]

Elliott KL, Houston DW, DeCook R and Fritzsch B (2015a) Ear manipulations reveal a critical period for survival and dendritic development at the single-cell level in Mauthner neurons. Developmental Neurobiology, 75(10), 1339–1351. [PubMed: 25787878]

Elliott KL, Houston DW and Fritzsch B (2015b) Sensory afferent segregation in three-eared frogs resemble the dominance columns observed in three-eyed frogs. Scientific reports, 8, 8338.

Elliott KL, Houston DW and Fritzsch B (2013) Transplantation of Xenopus laevis tissues to determine the ability of motor neurons to acquire a novel target. PLoS One, 8, e55541. [PubMed: 23383335]

Elliott KL, Kersigo J, Pan N, Jahan I and Fritzsch B (2017) Spiral ganglion neuron projection development to the hindbrain in mice lacking peripheral and/or central target differentiation. Frontiers in Neural Circuits, 11, 25. [PubMed: 28450830]

Fritzsch B (1993) Fast axonal diffusion of 3000 molecular weight dextran amines. Journal of Neuroscience Methods, 50, 95–103. [PubMed: 7506342]

Fritzsch B (1999) Hearing in Two Worlds: Theoretical and Actual Adaptive Changes of the Aquatic and Terrestrial Ear for Sound Reception In: Fay RR, Popper AN (eds) Comparative Hearing: Fish and Amphibians. Springer Handbook of Auditory Research, vol 11 Springer, New York, NY

Fritzsch B (1999) Hearing in two worlds: theoretical and actual adaptive changes of the aquatic and terrestrial ear for sound reception In Comparative hearing: fish and amphibians. New York: Springer, pp. 15–42.

Fritzsch B, Barald KF and Lomax MI (1998a) Early embryology of the vertebrate ear In Development of the auditory system. New York: Springer, pp. 80–145.

Fritzsch B, Barbacid M and Silos-Santiago I (1998b) Nerve dependency of developing and mature sensory receptor cells. Annals of the New York Academy of Sciences, 855, 14–27. [PubMed: 9929583]

Fritzsch B, Duncan JS, Kersigo J, Gray B and Elliott KL (2016a) Neuroanatomical tracing techniques in the ear: history, state of the art, and future developments In Sokolowski B (Ed.), Auditory and vestibular research: methods and protocols. New York: Springer, pp. 221–246.

Fritzsch B and Elliott KL (2017) Gene, cell, and organ multiplication drives inner ear evolution. Developmental Biology, 431, 3–15. [PubMed: 28866362]

Fritzsch B, Gregory D and Rosa-Molinar E (2005a) The development of the hindbrain afferent projections in the axolotl: evidence for timing as a specific mechanism of afferent fiber sorting. Zoology (Jena), 108, 297–306. [PubMed: 16351978]

Fritzsch B, Kersigo J, Yang T, Jahan I and Pan N (2016b) Neurotrophic factor function during ear development: expression changes define critical phases for neuronal viability, In The primary auditory neurons of the mammalian cochlea. New York: Springer, pp. 49–84.

Fritzsch B, Muirhead KA, Feng F, Gray BD and Ohlsson-Wilhelm BM (2005b) Diffusion and imaging properties of three new lipophilic tracers, NeuroVue Maroon, NeuroVue Red and NeuroVue Green and their use for double and triple labeling of neuronal profile. Brain research bulletin, 66, 249–258. [PubMed: 16023922]

Fritzsch B, Pan N, Jahan I and Elliott KL (2015) Inner ear development: building a spiral ganglion and an organ of corti out of unspecified ectoderm. Cell and Tissue Research, 361, 7–24. [PubMed: 25381571]

Fritzsch B, Pauley S, Feng F, Matei V and Nichols D, 2006 The molecular and developmental basis of the evolution of the vertebrate auditory system. International Journal of Comparative Psychology 19.

Fritzsch B, Sarai P, Barbacid M and Silos-Santiago I (1997) Mice with a targeted disruption of the neurotrophin receptor trkB lose their gustatory ganglion cells early but do develop taste buds. International Journal of Developmental Neuroscience, 15, 563–576. [PubMed: 9263033]

Gensberger KD, Kaufmann AK, Dietrich H, Branoner F, Banchi R, Chagnaud BP, et al. (2016) Galvanic vestibular stimulation: cellular substrates and response patterns of neurons in the vestibulo-ocular network. The Journal of Neuroscience, 36(35), 9097–9110. [PubMed: 27581452]

Giorgi P and Van der Loos H (1978) Axons from eyes grafted in Xenopus can grow into the spinal cord and reach the optic tectum. Nature, 275(5682), 746–748. [PubMed: 703840]

Glover JC, Elliott KL, Erives A, Chizhikov VV and Fritzsch B (2018) Wilhelm His' lasting insights into hindbrain and cranial ganglia development and evolution. Developmental Biology.

Goodrich LV (2016) Early development of the spiral ganglion In Dabdoub A, Fritzsch B, Popper AN and Fay RR (Eds.), The Primary Auditory Neurons of the Mammalian Cochlea. New York: Springer pp. 11–48.

Goto F, Straka H and Dieringer N (2001) Postlesional vestibular reorganization in frogs: evidence for a basic reaction pattern after nerve injury. Journal of Neurophysiology, 85, 2643–2646. [PubMed: 11387410]

Hallböök F, Wilson K, Thorndyke M and Olinski RP (2006) Formation and evolution of the chordate neurotrophin and Trk receptor genes. Brain, Behavior and Evolution, 68, 133–144.

Harrison RG, 1935 The Croonian lecture: on the origin and development of the nervous system studied by the methods of experimental embryology. Proceedings of the Royal Society of London. Series B, Biological Sciences, 118(808), 155–196.

Hernandez-Miranda LR, Müller T and Birchmeier C (2016) The dorsal spinal cord and hindbrain: from developmental mechanisms to functional circuits. Developmental biology.

Jacobson AG (1963) The determination and positioning of the nose, lens and ear. I. Interactions within the ectoderm, and between the ectoderm and underlying tissues. Journal of Experimental Zoology Part A: Ecological Genetics and Physiology, 154, 273–283.

Jahan I, Kersigo J, Pan N and Fritzsch B (2010) Neurod1 regulates survival and formation of connections in mouse ear and brain. Cell and Tissue Research, 341, 95–110. [PubMed: 20512592]

Klein S and Graziadei P (1983) The differentiation of the olfactory placode in Xenopus laevis: a light and electron microscope study. Journal of Comparative Neurology, 217, 17–30. [PubMed: 6875050]

Kopecky BJ, Duncan JS, Elliott KL and Fritzsch B (2012) Three-dimensional reconstructions from optical sections of thick mouse inner ears using confocal microscopy. Journal of Microscopy, 248, 292–298. [PubMed: 23140378]

Korn H and Faber DS (2005) The Mauthner cell half a century later: a neurobiological model for decision-making? Neuron, 47, 13–28. [PubMed: 15996545]

Kullander K and Klein R (2002) Mechanisms and functions of eph and ephrin signalling. Nature Reviews Molecular Cell Biology, 3, 475–486. [PubMed: 12094214]

Lai HC, Seal RP and Johnson JE (2016) Making sense out of spinal cord somatosensory development. Development, 143(19), 3434–3448. [PubMed: 27702783]

Lambert FM, Beck JC, Baker R and Straka H (2008) Semicircular canal size determines the developmental onset of angular vestibuloocular reflexes in larval Xenopus. The Journal of Neuroscience: The official Journal of the Society for Neuroscience, 28(32), 8086–8095. [PubMed: 18685033]

Liu Z, Hamodi AS and Pratt KG (2016) Early development and function of the Xenopus tadpole retinotectal circuit. Current Opinion in Neurobiology, 41, 17–23. [PubMed: 27475307]

Magrassi L and Graziadei P (1985) Interaction of the transplanted olfactory placode with the optic stalk and the diencephalon in Xenopus laevis embryos. Neuroscience, 15, 903–921. [PubMed: 4069358]

Maklad A and Fritzsch B (2003) Development of vestibular afferent projections into the hindbrain and their central targets. Brain Research Bulletin, 60, 497–510. [PubMed: 12787869]

Manns M and Fritzsch B (1991) The eye in the brain: retinoic acid effects morphogenesis of the eye and pathway selection of axons but not the differentiation of the retina in Xenopus laevis. Neuroscience letters, 127, 150–154. [PubMed: 1881624]

Mao Y, Reiprich S, Wegner M and Fritzsch B (2014) Targeted deletion of Sox10 by Wnt1-cre defects neuronal migration and projection in the mouse inner ear. PLoS ONE, 9, e94580. [PubMed: 24718611]

Mombaerts P, Wang F, Dulac C, Chao SK, Nemes A, Mendelsohn M, et al. (1996) Visualizing an olfactory sensory map. Cell, 87, 675–686. [PubMed: 8929536]

Morrison EE and Graziadei PP (1983) Transplants of olfactory mucosa in the rat brain I. A light microscopic study of transplant organization. Brain Research, 279, 241–245. [PubMed: 6640344]

Nieuwkoop P and Faber J (1994) Normal table of Xenopus Laevis (Daudin): a systematical and chronological survey of the development from the fertilized egg till the end of metamorphosis. New York: Garland Publishing.

Patel AV, Huang T and Krimm RF (2010) Lingual and palatal gustatory afferents each depend on both BDNF and NT-4, but the dependence is greater for lingual than palatal afferents. Journal of Comparative Neurology, 518(16), 3290–3301. [PubMed: 20575060]

Rohregger M and Dieringer N (2003) Postlesional vestibular reorganization improves the gain but impairs the spatial tuning of the maculo-ocular reflex in frogs. Journal of Neurophysiology, 90, 3736–3749. [PubMed: 12890798]

Sperry RW (1963) Chemoaffinity in the orderly growth of nerve fiber patterns and connections. Proceedings of the National Academy of Sciences, 50, 703–710.

Stout R and Graziadei P (1980) Influence of the olfactory placode on the development of the brain in Xenopus laevis (Daudin): I. Axonal growth and connections of the transplanted olfactory placode. Neuroscience, 5(12), 2175–2186. [PubMed: 7465050]

Straka H, Fritzsch B and Glover JC (2014) Connecting ears to eye muscles: evolution of a ‘simple’ reflex arc. Brain, Behavior and Evolution, 83, 162–175.

Straka H and Simmers J (2012) Xenopus laevis: an ideal experimental model for studying the developmental dynamics of neural network assembly and sensory-motor computations. Developmental Neurobiology, 72, 649–663. [PubMed: 21834082]

Swanson GJ, Howard M and Lewis J (1990) Epithelial autonomy in the development of the inner ear of a bird embryo. Developmental biology, 137, 243–257. [PubMed: 2303163]

Tonniges J, Hansen M, Duncan J, Bassett M, Fritzsch B, Gray B, et al. (2010) Photo-and bio-physical characterization of novel violet and near-infrared lipophilic fluorophores for neuronal tracing. Journal of microscopy, 239, 117–134. [PubMed: 20629917]

Yang T, Kersigo J, Wu S, Fritzsch B and Bassuk AG (2017) Prickle1 regulates neurite outgrowth of apical spiral ganglion neurons but not hair cell polarity in the murine cochlea. PLoS ONE, 12, e0183773. [PubMed: 28837644]

Yntema C (1955) Ear and nose. Analysis of Development, 415–428.

Zarei K, Elliott KL, Zarei S, Fritzsch B and Buchholz JHJ (2017) A method for detailed movement pattern analysis of tadpole startle response. Journal of the Experimental Analysis of Behavior, 108, 113–124. [PubMed: 28653338]

Zecca A, Dyballa S, Voltes A, Bradley R and Pujades C (2015) The order and place of neuronal differentiation establish the topography of sensory projections and the entry points within the hindbrain. Journal of Neuroscience, 35(19), 7475–7486. [PubMed: 25972174]

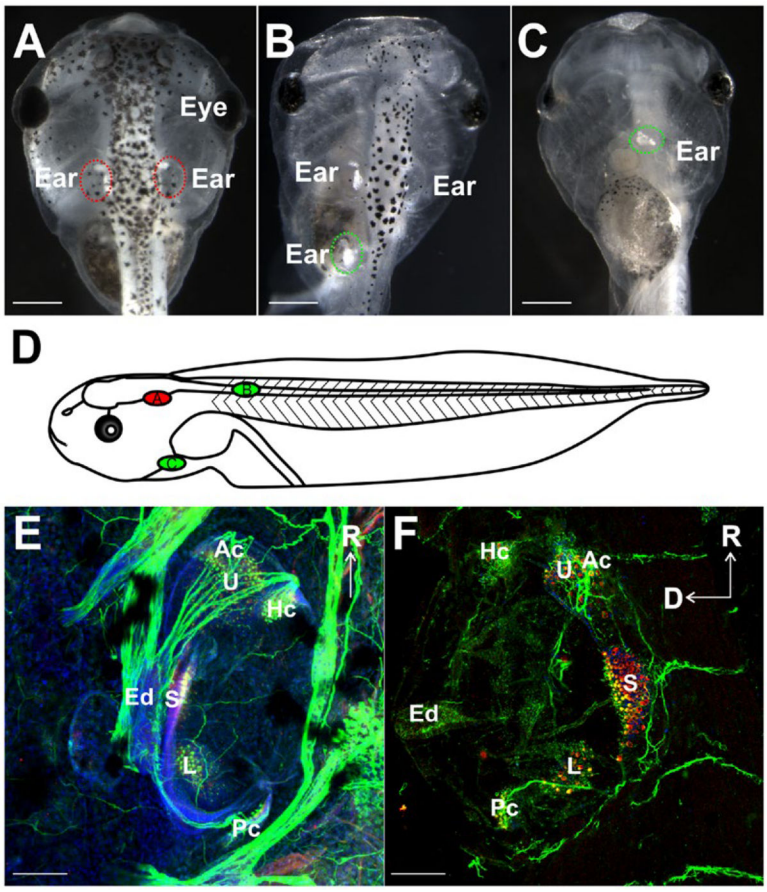

Figure 1.

Evaluation of ear transplantations (A–D) Stage 46 *X. laevis* embryos showing positions of native ears and transplanted ears (circled). (A) Control animal. (B) Embryo with a third ear transplanted adjacent to the spinal cord. (C) Ventral view of embryo with a third ear transplanted next to the heart. (D) Schematic diagram representing a lateral view of stage 46 *X. laevis* demonstrating the positions of the native ear (red, A) and the two different transplantations (green, B,C). (E) Control ear and (F) a transplanted ear labeled with antibodies against MyoVI (red) and tubulin (green) demonstrating the presence of hair cells in six distinct epithelia along with Hoechst nuclei counterstain (blue) (Utricle, U; Saccule, S; Lagena, L; Anterior canal, Ac; Horizontal canal, Hc; Posterior canal, Pc) and neurons, respectively. Endolymphatic duct is labeled Ed. Scale bars in A–C are 0.5 mm and 100 μm in E–F Rostral, R; Dorsal, D. [Colour figure can be viewed at wileyonlinelibrary.com]

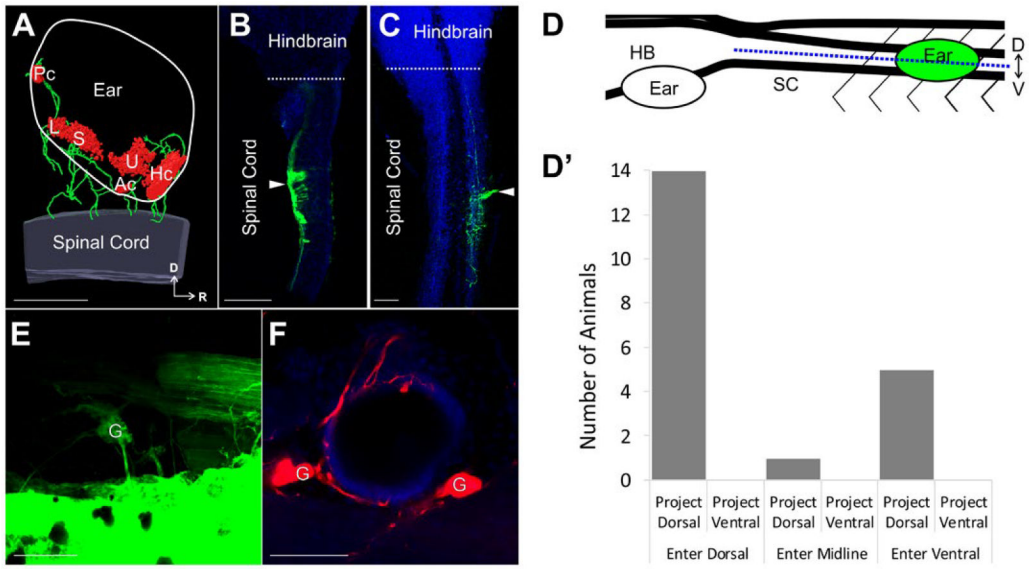

Figure 2.

Ear afferent innervation of the spinal cord (A) 3D reconstruction of an ear transplanted adjacent to the spinal cord labeled with antibodies against Tubulin (green) and MyoVI (red) displaying neurons and hair cells, respectively. (B–C) Single optical sections of an *X. laevis* brain and spinal cord (blue, autofluorescence) in the dorsal (B) and ventral (C) plane following injection of dye (green) into an adjacently transplanted ear shows afferents entering the spinal cord dorsally and ventrally, respectively. White arrowhead indicates the entry point of inner ear afferent projections. (D) Lateral view schematic diagram showing the position of the transplanted ear and the defined midline position (blue dotted line) along the dorsal-ventral axis of the spinal cord used to assign entry and projection planes of labeled afferents in B–C. (D′) Analysis of entry point and plane of projection for animals with ears transplanted adjacent to the spinal cord. Serial optical sections were analyzed for entry point of labeled fibers (dorsal, midline, ventral) and for plane of projection (dorsal, ventral). $n = 20$. (E) Backfilling of inner ear ganglion cells in an ear adjacent to the spinal cord from dye injection into the spinal cord rostral to the transplanted ear. (F) Backfilling (red) of inner ear ganglia and peripheral afferent processes on hair cells in an ear adjacent to the spinal cord from dye injection into the spinal cord. Hoechst nuclei counterstained in blue. Spinal Cord, SC; Hindbrain, HB; Dorsal, D; Ventral, V; Rostral, R; Ganglion cells, G; Utricle, U; Saccule, S; Lagena, L; Anterior canal, Ac; Horizontal canal, Hc; Posterior canal, Pc. Scale bars are 100 μm. [Colour figure can be viewed at wileyonlinelibrary.com]

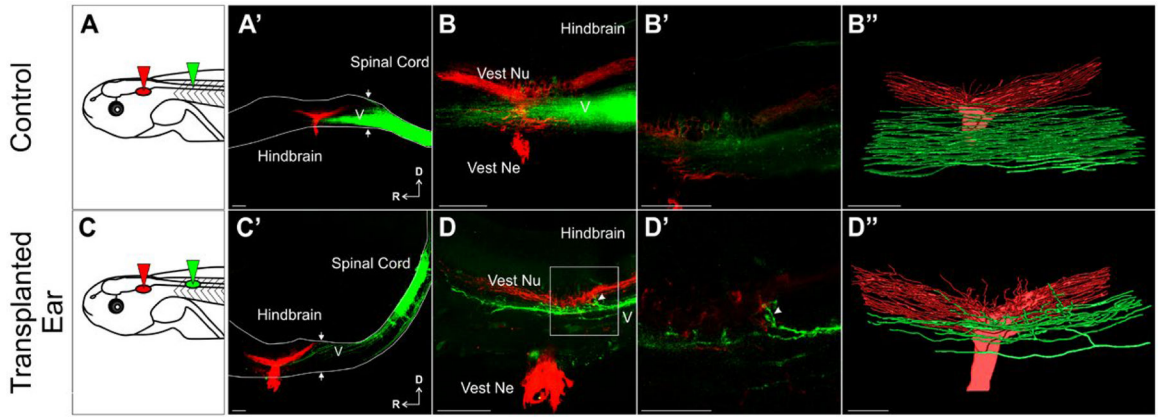

Figure 3.

Afferent innervation of the hindbrain by ears transplanted adjacent to the spinal cord (A) Schematic of dye placement for control animals. (A′) Control hemisection of the brain and spinal cord showing ascending spinal fibers (green) enter the hindbrain and fill the descending tract of trigeminal nucleus (V, unlabeled). Native ear projections (red) into the vestibular nucleus in the hindbrain are labeled. Note the lack of overlap between the trigeminal nucleus and vestibular nucleus at higher magnification of A′ (B) and of B, shown as a single optical section (B′). (B″) 3D reconstruction of entire stack in B. (C) Schematic of dye placement for animals with ears transplanted adjacent to the spinal cord. (C′) Hemisection showing ascending spinal tracts and spinal cord transplanted ear afferent fibers projecting into the hindbrain (green) along the descending tract of V (unlabeled). (D) Higher magnification of C′ showing inner ear afferents projecting into the vestibular nucleus from the trigeminal nucleus (arrowhead). (D′) Higher magnification of box in D showing projections into the vestibular nucleus (arrowhead) in a single optical section. (D″) 3D reconstruction of entire stack in D. 8 experimental animals were analyzed. Arrows denote the hindbrain/spinal cord boundary. Scale bars are 100 μm in A′, B, B″, C′, C″, D and 50 μm in B′, D′. Vest Ne vestibular nerve, Vest Nu vestibular nucleus, D dorsal, R rostral. [Colour figure can be viewed at wileyonlinelibrary.com]

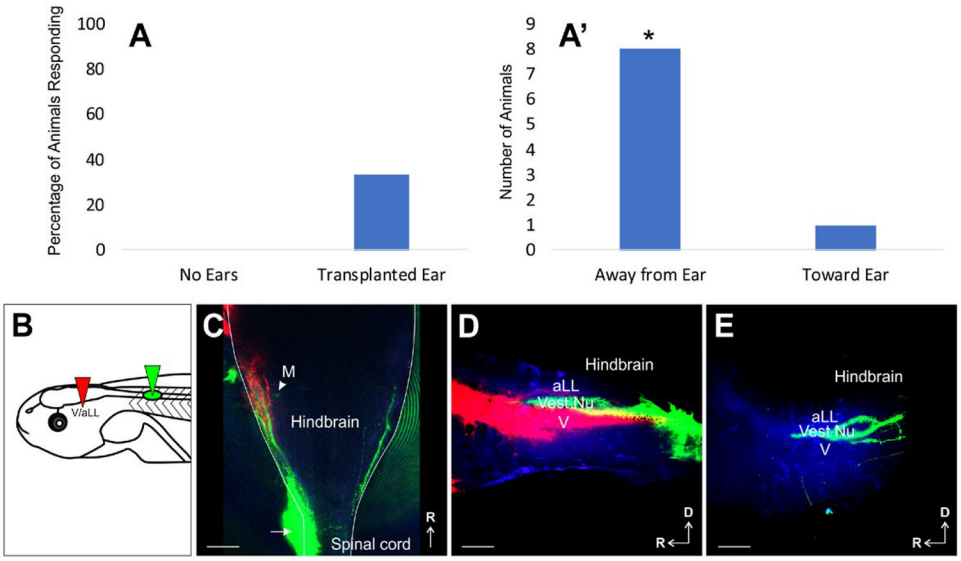

Figure 4.

C-Start Startle Response by Transplanted Ears. (A) Percentage of animals that displayed a C-start startle response following stimulation in control animals with no ears and in animals in which the only ear was the transplanted ear adjacent to the spinal cord. (A′) Direction in each trial with a positive response observed in A from animals in which the only ear was the transplanted ear adjacent to the spinal cord. $*P < 0.05$, Chi-Square analysis. (B) Schematic of dye placement. (C) Whole-mount of a hindbrain from an animal that had a response in all four trials, three were in the direction away from the transplanted ear and one in the direction toward the transplanted ear. Arrow designates entry point of transplanted inner ear afferents. M, Mauthner cell. (D) Lateral view of ipsilateral hemisected hindbrain showing projections of transplanted ear afferents (green) in between anterior lateral line (aLL) and trigeminal (V) afferent central projections (red). (E) Lateral view of contralateral hemisected hindbrain showing projections of a transplanted ear afferents (green) in between the region where the anterior lateral line (aLL) and trigeminal (V) nuclei are located. Autofluorescence is in blue. Scale bars are 100 μm. [Colour figure can be viewed at wileyonlinelibrary.com]

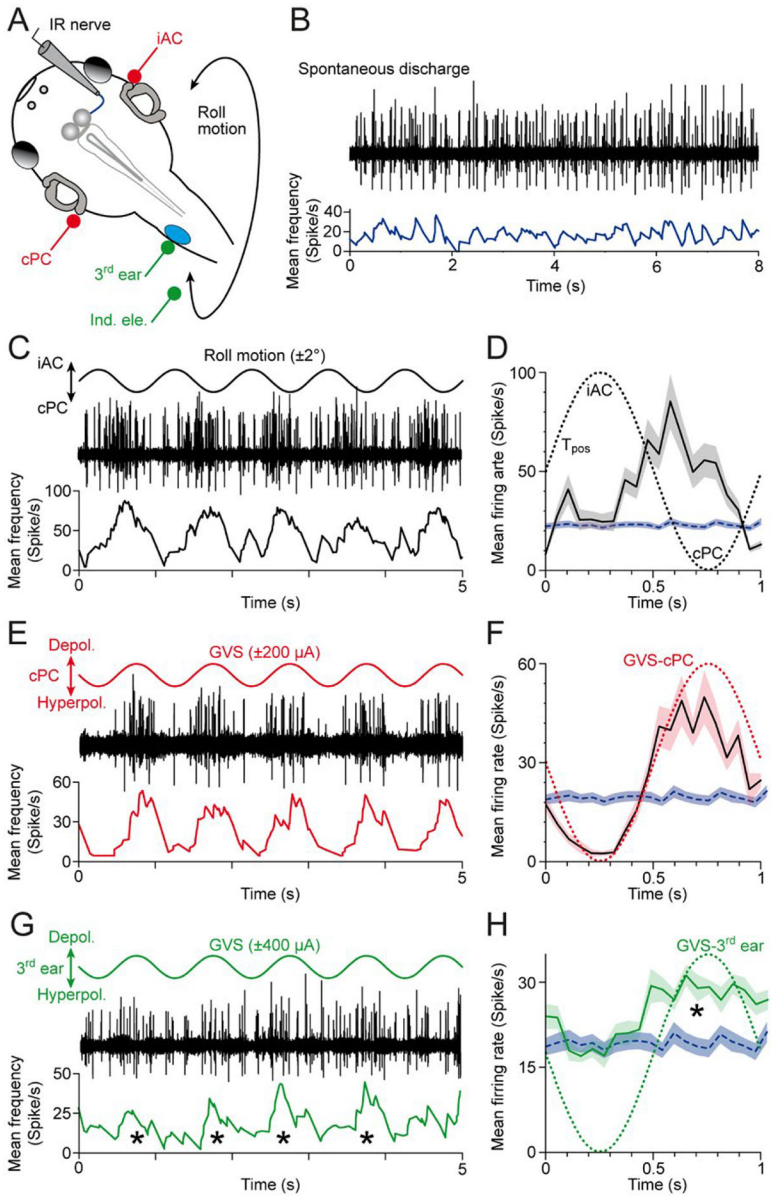

Figure 5.

Multi-unit inferior rectus (IR) nerve discharge during activation of native bilateral semicircular canals and a transplanted third ear on the spinal cord. (A) Schematic of a semi-intact *Xenopus* preparation depicting the recording of the right IR nerve during roll motion (black curved double arrow), galvanic vestibular stimulation (GVS) of the contralateral posterior (cPC) and iAC semicircular canal epithelia (iAC; red electrodes) and of the transplanted third ear (green electrodes). (B) Episode of spontaneous IR nerve discharge (black trace) with an average resting rate of ~20 spikes/s (blue trace) in an isolated preparation obtained from a stage 55 tadpole. (C, E, G) Modulated multi-unit discharge (black traces) and mean firing rate (lower colored traces) of the same IR nerve during roll motion in the cPC-iAC plane (C), during GVS of the cPC-iAC (E) and during GVS of the third ear (G); sinusoids indicate the waveform (1 Hz) for natural and galvanic stimulation.

(D, F, H) Modulated mean IR nerve firing rate over a single cycle (black traces) ± SEM (color-shaded areas) of the responses shown in C,E,G; the averages were obtained from 20–120 single cycles, respectively; the colored dotted sinusoids indicate the motion stimulus (D) and GVS of the cPC (F) and third ear (H), and the blue dashed line and horizontal band the mean ± SEM resting rate of the IR nerve. Note that the IR nerve increases firing during motion in direction of the cPC (D), galvanic depolarization of the cPC epithelium (F) and galvanic depolarization of the third ear (*in G, H). T_{pos}, position signal of the turntable. [Colour figure can be viewed at wileyonlinelibrary.com]

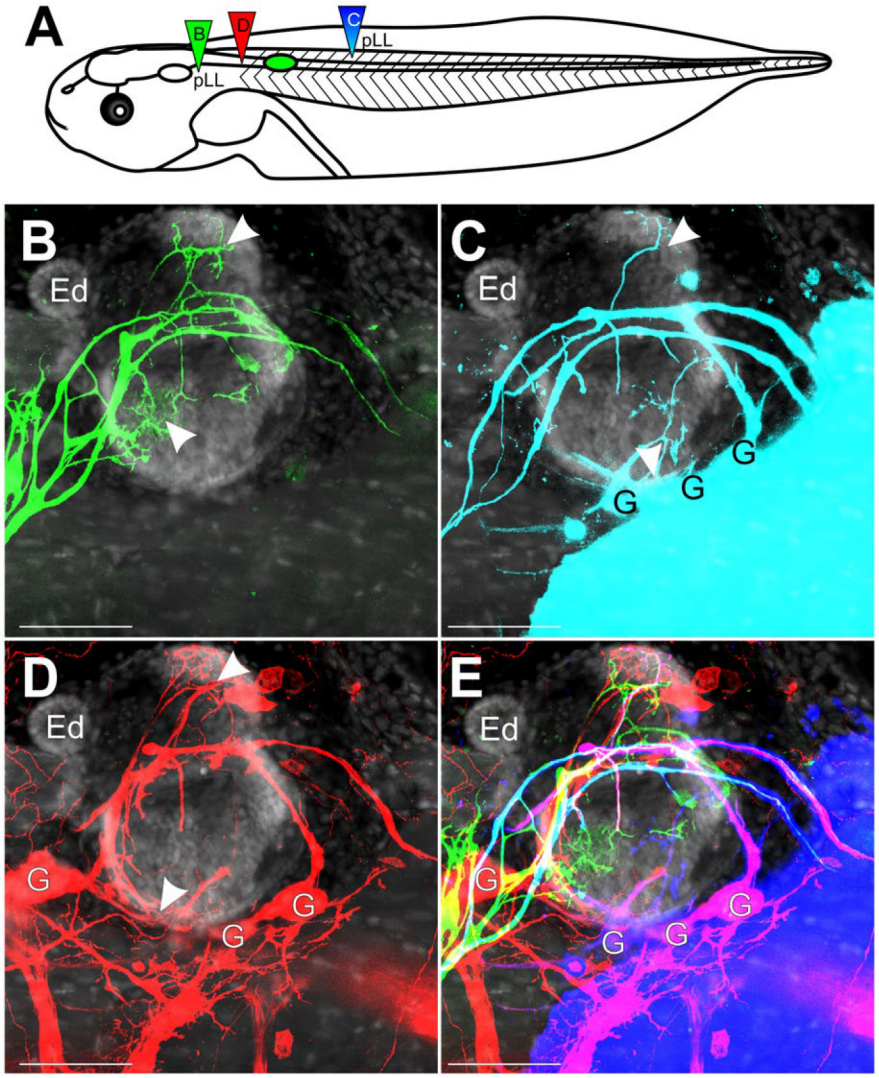

Figure 6.

Inner Ear Afferent Fasciculation with Lateral Line. (A) Schematic of dye placement for the different transplants. (B) Lateral view of afferents of the pLL projecting over and into the ear (green, dye injection B in panel A). The ear was transplanted adjacent to the spinal cord at stage 32–36. No ganglia were labeled. (C) Lateral view of pLL and inner ear afferents from a caudal dye injection into caudal portion of the pLL nerve (cyan, dye injection C in panel A). G, ganglia. (D) Lateral view of inner ear afferents from a spinal cord injection rostral to the transplanted ear (red, dye injection D in panel A) G, ganglia. (E) Merge of B-D. Cyan of panel C has been replaced by blue. Panels B–E are counterstained for nuclei marker Hoechst (gray). Arrowheads indicate areas of innervation of the inner ear. Scale bars are 100 μm. Endolymphatic duct, Ed. [Colour figure can be viewed at wileyonlinelibrary.com]

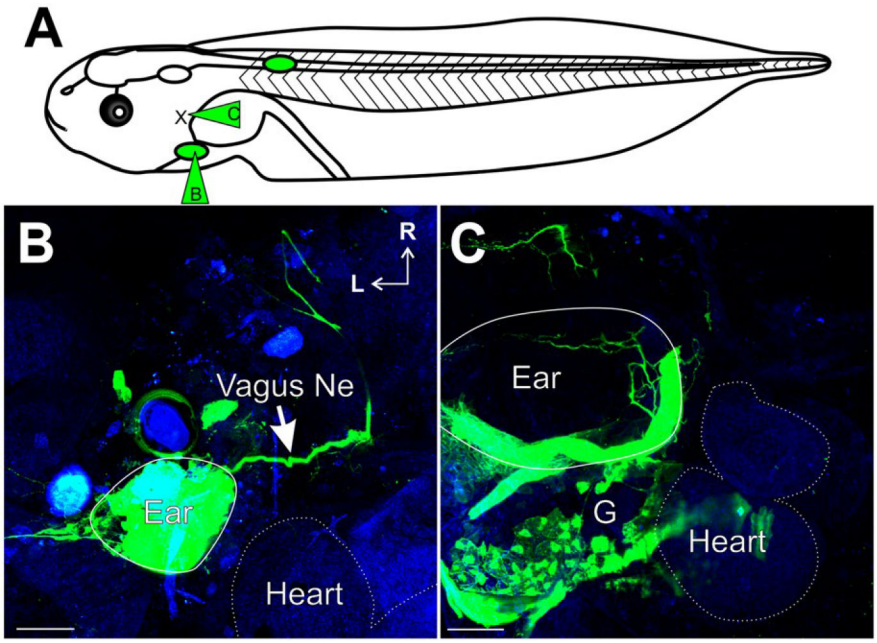

Figure 7.

Inner Ear Afferent Fasciculation with the Vagus nerve. (A) Schematic of ear transplants showing dye placement for the ears transplanted adjacent to the heart. (B) Ventral view of an animal with an ear transplanted into the heart region showing ear afferents projecting with the vagus nerve (green, dye injection B in panel A; Vagus Ne, arrow). Heart is outlined with a dotted line as determined from autofluorescence background (blue). (C) Ventral view of an animal with an ear transplanted next to the heart. Labeling (green) from dye injection into the vagus nerve (dye injection C in panel A) showing innervation of the ear and labeling of inner ear ganglia. Autofluorescense background (blue). Scale bars are 100 μm. Rostral, R; Lateral, L. [Colour figure can be viewed at wileyonlinelibrary.com]

Table 1

Success of Transplantations

Location of transplantation	Development with otoconia	Development without otoconia	No ear development
Adjacent to Spinal Cord Early[a] (117)	98	11	8
Adjacent to Spinal Cord Late[b] (45)	36	1	8
Adjacent to Heart (25)	21	0	4

[a] Early is defined as transplantations occurring during stages 25–27.

[b] Late is defined as transplantations occurring during stages 28–36.